Int. J. Electrochem. Sci., 6 **(2011)** 5396 - 5416

International Journal of ELECTROCHEMICAL SCIENCE
www.electrochemsci.org

Corrosion Inhibition of Mild Steel in Near Neutral Solution by *Kraft* and *Soda Lignins* Extracted from Oil Palm Empty Fruit Bunch

Ebrahim Akbarzadeh, M. N. Mohamad Ibrahim[*], *Afidah Abdul Rahim*

Lignocellulosic Research Group, School of Chemical Sciences, Universiti Sains Malaysia, 11800 Penang, Malaysia
[*]E-mail: mnm@usm.my

Received: 6 August 2011 / *Accepted:* 28 September 2011 / *Published:* 1 November 2011

Lignin is the second most natural organic polymer on the earth and it can be acquired from the wastes of wood pulping processing in the form of black liquor. The inhibition efficiencies of Kraft lignin (KL) and Soda lignin (SL) on the corrosion of mild steel in 3.5% (w/v) sodium chloride at two levels of pH have been evaluated by weight loss method, electrochemical techniques and surface analysis using 50-800 ppm (w/v) inhibitor concentration at 25 °C. Both KL and SL can perform as good inhibitors for the above-mentioned system. The KL gave maximum inhibition efficiencies of 95 and 92% for pH 6 and pH 8, respectively at high concentrations of inhibitor, whereas SL gave 97 and 95% inhibition efficiencies for pH 6 and pH 8, respectively at 800 ppm of inhibitor concentration. Polarization studies confirmed that KL and SL are mixed type inhibitors. Both KL and SL obey Langmuir's adsorption isotherm at two levels of pH and 25 °C. FT-IR and surface analyses confirmed that the surface of mild steel was affected by the adsorption of lignin onto the surface to form ferric-lignin compounds. The rust components especially lepidocrocite were reduced; hence, lignin can be used as a rust converter.

Keywords: *Kraft lignin, Soda lignin*, Corrosion inhibitor, Sodium chloride, Adsorption

1. INTRODUCTION

Corrosion inhibitors are used as effective alternatives for the protection of metallic surfaces against corrosion. Most synthetic corrosion inhibitors produce hazardous effects for the environment and operators of most synthetic corrosion inhibitors. Despite their high inhibition efficiency and good protection for metals, their toxicity and carcinogenic properties are significant. Both are valid reasons for this study; the health and environmental friendliness of natural materials. Plant compounds have been recently studied as corrosion inhibitors for different metals in various environments. Perhaps, the most common natural substances used are plant extracts, such as tannin extracts [1], vanillin [2],

Opuntia extracts [3], natural honey [4], lupine extract [5], and other plant extracts [6] that possess an active functional group, such as nitro (-NO_2) or a hydroxyl (-OH) groups [7]. Literature reviews on corrosion inhibitors have shown that organic inhibitors contain nitrogen, oxygen, sulphur or aromatic rings in their molecular structure. Corrosion inhibition efficiency increases in the sequence of O<N<S<P [8-10].

Lignin may be the second most abundant natural organic polymer on earth [11]. Lignin is a heterogeneous biopolymer and a chemical compound that is an integral part of plant cell walls which provides the mechanical strength of plants cellulose [12]. Lignin is assembled from coniferyl alcohol type monomers by enzymatic polymerization providing a three-dimensional molecular architecture. Lignin can be extracted from both hardwood and softwood via a variety of ways of wood pulping in various solvents. Naturally, lignin is a hydrophobic molecule but it can be dissolved in water gradually by increasing the pH. Different types of lignin can be isolated depending on the extraction methods. Kraft pulping and soda pulping using sodium sulfide and sodium hydroxide, respectively are the most common technique to produce lignin. Malaysia has more than 2.5 million hectares of palm oil plantations that produce about 30 million tons of empty fruit bunches (EFB) generated from palm oil milling operations annually. The oil palm empty fruit bunch (EFB) can be one of the alternative sources of lignin (around 20% w/w) that can be derived from waste material and at the same time help to preserve natural treasures for future generations. Eight monomers were identified in lignin that was extracted from EFB.

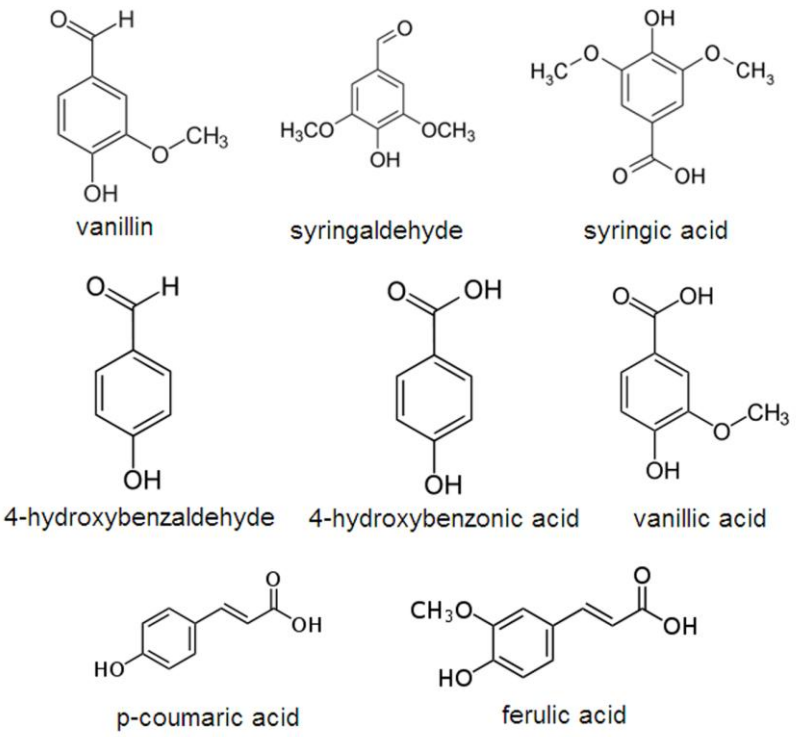

Figure 1. The monomer structures of lignin.

They are (Fig. 1) vanillin, syringaldehyde, syringic acid, 4-hydroxybenzaldehyde, 4-hydroxybenzonic acid, vanillic acid, p-coumaric acid and ferulic acid [13].

The inhibition efficiency of corrosion inhibitors have been reported by several researchers on the corrosion of mild steel in NaCl medium by various natural organic compounds [14, 15]. Most natural organic substances can be adsorbed on the exposed corroding surfaces and decrease the corrosion rate, shifting the polarization curves to anodic oxidation or cathodic reduction regions, whereby giving us anodic, cathodic or a mixed type of inhibition.

In this study, the inhibitive and rust converter potential of Kraft lignin (KL) and soda lignin (SL) on the corrosion of mild steel in 3.5% NaCl solution have been investigated at various concentrations of inhibitors at two different levels of pH conducted by the weight loss method and the electrochemical tests. The nature of inhibitor adsorption mechanism, formation of new phase onto the metal surface and morphology as well as chemical content of corroded metal surface were also studied and discussed.

2. EXPERIMENTAL

2.1 Materials used

The natural soda and Kraft lignin had been extracted from the black liquor (Black liquor is the spent cooking liquor when digesting pulpwood into paper pulp; removing lignin, hemicelluloses and other extractive materials from the wood to free the cellulose fibers) of oil palm empty fruit bunch by adding 20% (v/v) sulphuric acid in order to reach pH 2.

After filtering and washing, the extracted lignins were dried at 45 °C for 3 days and then was ground (<200 μm) carefully [16].

Mild steel was used throughout the experiments with the chemical composition as shown in Table 1. The rectangular mild steel coupons of size 2.5 cm×2.5 cm×0.25 cm were used.

Table 1 Chemical composition (wt %) of carbon steel tested

Element	C	S	Si	P	Mn	Fe
% composition (w/w)	0.2	0.047	0.06	0.039	0.55	remainig

2.2 Solution preparation

The reference solutions were prepared from 800 ppm (w/v) of soda and Kraft lignins that were diluted to reach concentrations of 400, 200, 100 and 50 ppm (w/v) in 3.5% w/v of sodium chloride. Finally, the pH was adjusted to the favored pH 6 and 8 by adding 0.1 M NaOH. All reagents used in these experiments were prepared from analytical grade reagents. The test solutions for all trials were quiescent and at 25 °C under naturally aerated conditions. Three monomers of lignin namely p-cumaric

acid (CA), ferulic acid (FA) and 4-hydroxybenzaldehyde (HB)) were selected based on percentage content in lignin and solubility in water. Four different levels of concentrations (800, 400, 200 and 100 ppm) of each monomer and 3.5% NaCl were used for the preparation of solutions for the potentiodynamic analysis.

2.3 Weight loss measurements

The mild steel coupons were first abraded with emery paper of different grades, 200 and 400, degreased with ethanol, washed with distilled water and dried under a flow of air. Finally, they were accurately weighed before immersing in the test solution as per standard procedures [17]. The loss of mass was measured for 10 consecutive days or equivalent to 240 hours containing various concentrations of inhibitors mentioned previously. Following the immersion, the specimens were taken out, washed with distilled water, dried and re-weighed. The corrosion rate (C_r, mpy) and the inhibition efficiency (%*IE*) can be calculated by the following expressions from the weight loss measurements [18, 19]:

$$C_r(\text{mpy}) = \frac{534 \times w}{At\rho} \quad (1)$$

where w is the corrosion weight loss of mild steel (mg), A is the exposure area (cm^2), t is the exposure time (hours) and ρ is the density of mild steel (g cm^{-3}). The percentage of inhibition efficiency, %*IE* is given by [20]:

$$\%IE = \frac{w_0 - w_i}{w_0} \times 100 \quad (2)$$

where w_0 and w_i are the corrosion weight loss of mild steel in uninhibited and inhibited conditions, respectively.

2.4 Potentiodynamic polarization measurements

The electrochemical experiments were carried out using a conventionally designed three-electrode glass cell of Gamry Potentiostat/Galvanostat (Reference R600™) with a software package from Framework® Gamry-Instruments Inc., USA. The potentiodynamic curves were plotted over a potential range of -900 mV to -500 mV with respect to open circuit potential (E_{ocp}) at a scan rate of 1 mV s^{-1}. The platinum electrode as a counter electrode and a standard calomel electrode (SCE) as a reference electrode were employed in these experiments. Mild steel samples which were located at the bottom of the cell with an exposure area of 3.14 cm^2 were used as a working electrode. Various corrosion kinetic parameters such as corrosion current density (i_{corr}), corrosion potential (E_{corr}), anodic and cathodic Tafel slopes (b_a, b_c) were obtained at pH 6 and 8. Corrosion current density can be

measured by the intersection of the extrapolated Tafel lines to the E_{corr} of the mild steel electrode. The inhibition efficiency can be calculated from the following equation [21].

$$\%IE = \left[\frac{(i^0_{corr} - i_{corr})}{i^0_{corr}} \right] \times 100 \quad (3)$$

Where i^0_{corr} and i_{corr} are uninhibited and inhibited corrosion current densities, respectively.

2.5 Electrochemical impedance measurements

The impedance measurements were carried out by using the same instrument and cell's arrangement (three-electrode glass cell) mentioned above. The Echem analyst software of Gamry Instrument was used for analyzing and the calculation of elements in the equivalent circuits. E_{ocp} of sample was immersed for 30 min over a frequency range of 100 kHz to 5 mHz with a signal amplitude perturbation of 10 mV and scan rate of 1 mV s^{-1}. The equivalent circuit was proposed and the values of elements of the circuit can be measured from Nyquist plots. The charge transfer resistance, R_{ct} and double layer capacitance, C_{dl} values were then calculated.

2.6 Surface analyses

Scanning Electron Microscope (LEO SUPRA 55VP FESEM), which was equipped with an energy dispersive X-ray microanalysis (EDX) system (Oxford INCA 400) was used to study the morphology and chemical analysis of the corroded mild steel surfaces. FT-IR spectroscopy (Perkin-Elmer 2000 FTIR spectrometer) was used to collect the IR spectra of the mild steel corrosion products for the blank and containing high concentration inhibitor samples at two levels of pH 6 and 8.

3. RESULTS AND DISCUSSION

3.1 Weight loss measurements

The weight loss results of mild steel in 3.5% NaCl and various concentrations of SL and KL at 25 °C and two levels of pH 6 and 8 are given in Table 2. It can be observed that in most conditions, the corrosion rate values decreased and the inhibitor efficiency values increased with the increase of the SL and KL concentrations for both pH levels. But after a particular concentration of the inhibitors, the corrosion rate does not increase; moreover, the inhibitor efficiency remains constant with the increase of inhibitor concentration as seen in Fig. 2. The addition of SL and KL changed the corrosion rate and the inhibition efficiency considerably but there was not much different in the values of corrosion rate and the inhibitor efficiency by raising the concentration of inhibitors after 400 ppm at pH 6 and supposedly more than 1000 ppm of inhibitor concentration for pH 8.

Table 2 The weight loss results of immersion of steel samples in 3.5% NaCl without and with various concentrations of soda and Kraft lignin at pH 6 and 8.

Inhibitor Conc. (ppm)	**Weight loss (mg)**				**Corrosion rate (mpy)**				**%*IE***			
Inhibitor type	SL		KL		SL		KL		SL		KL	
pH	6	8	6	8	6	8	6	8	6	8	6	8
Blank	213	178	213	178	28.91	23.47	28.91	23.47	-	-	-	-
50	45	32	44	34	5.855	4.232	5.818	4.548	78.87	82.13	83.34	80.67
100	39	28	31	31	4.990	3.744	4.115	3.472	81.88	84.10	85.26	82.58
200	32	24	24	28	4.172	3.189	3.241	3.543	85	86.52	86.73	84.38
400	21	19	21	25	2.838	2.342	2.811	3.184	88.70	87.33	88.14	86.12
800	18	17	18	19	2.378	2.119	2.471	2.452	91.55	90.73	91.02	89.38

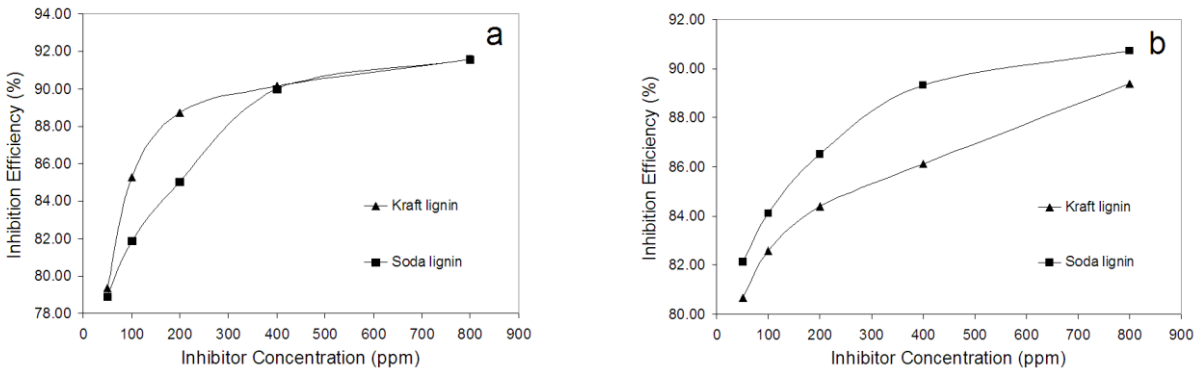

Figure 2. The inhibition efficiency of steel samples in 3.5% NaCl at various concentrations of soda lignin (SL) and Kraft lignin (KL) at (a) pH 6 and (b) pH 8.

Table 2 shows that the corrosion rate values decreased from 28.91 mpy to 2.37 mpy and 2.47 mpy at pH 6 for SL and KL, respectively. Similarly, corrosion rate values decreased from 23.47 mpy to 2.11 mpy and 2.45 mpy at pH 8 for SL and KL, respectively. The highest inhibition efficiencies around 91.55% and 90.73% were observed at pH 6 and 8, respectively for SL at the highest concentration. In the case of KL, the highest inhibition efficiencies of 90.73% and 89.38% were obtained at pH 6 and 8, respectively, at 800 ppm of the natural inhibitor. The increasing number of molecules of inhibitor covering the surface area of metal with the increase of its concentration resulted in a decrease of the corrosion rate and increase of inhibition efficiency. Generally it is assumed that the first step of the inhibition of aggressive media is the adsorption mechanism of the inhibitor at the metal/solution interface. Some types of adsorption of organic molecules at the metal/solution interface are mentioned by the following: (1) electrostatic interaction between the charged metal and the charged molecules, (2) interaction of uncharged electrons pairs in the inhibitor molecule with the metal surface, (3) interaction of π-electrons with the metal and (4) combination of (1) and (3) [22]. The

binding formation capability of a molecule with metal depends on the charge on the chelating atom. The chemisorption mechanism of adsorbing the inhibitor molecules involves the sharing or transfer of charge from the molecules to the surface to form a coordinate bond. Commonly, transition for metals having a vacant low energy electron orbital is electron transfer. For instance, the electron transfer can be expected with inhibitors having relatively loosely bound electrons [23, 24]. Lignins, consisting of polyphenolic monomers (Fig. 1) are expected to adsorb onto the metal due to the presence of the oxygen electron donating groups via the different adsorption modes described above.

3.2 Polarization curves

The potentiodynamic polarization curves of mild steel in 3.5% NaCl without and with various concentrations of SL and KL at pH 6 and 8 at 25 °C are shown in Fig. 3.

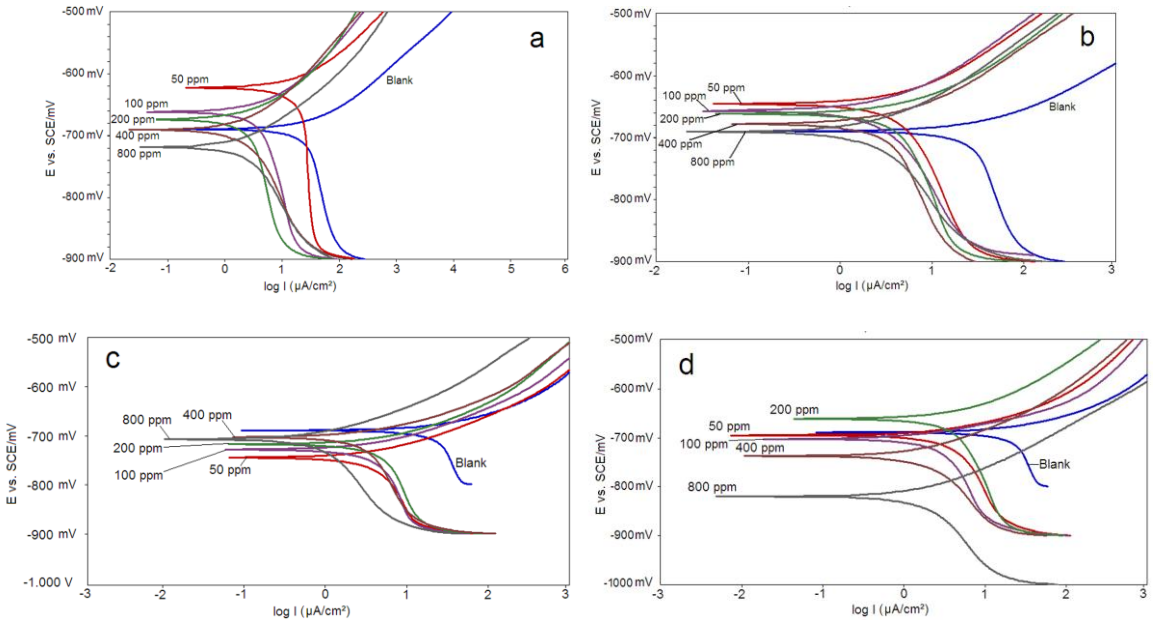

Figure 3 Polarization curves of mild steel in 3.5% NaCl, (a) SL, pH 6 (b) KL, pH 6 (c) SL, pH 8 (d) KL and pH 8.

The polarization parameters such as E_{corr}, I_{corr}, b_c, b_a, %*IE*, degree of surface coverage (θ) and inhibition coefficient (v) are obtained and given in Table 3 and 4 for both inhibitors at pH 6 and 8, respectively. Inhibitor efficiencies, %*IE* (Equation (3)), are calculated at different inhibitor concentrations from anodic and cathodic polarization curves (Fig. 3). The degree of surface coverage (θ) was calculated using the following Equation (4) [25]:

$$\theta = 1 - \frac{i_{corr}}{i^0_{corr}} \quad (4)$$

Inhibition coefficient (v) was calculated from Equation 5 [26]:

$$v = \frac{i^0_{corr}}{i_{corr}} \quad (5)$$

where i^0_{corr} and i_{corr} are the corrosion current densities in the uninhibited and inhibited solutions, respectively. The polarization resistance (R_p) was calculated using the Stern–Geary Equation (6) [27]:

$$R_p = \frac{b_c b_a}{2.303 i_{corr}(b_c + b_a)} \quad (6)$$

It can be observed from Table 3 that corrosion current density values decreased from 8.89 to 2.13 μA cm^{-2} and 8.15 to 3.16 μA cm^{-2} and the inhibitor efficiency increased from 79 to 95% and 81 to 92% with the increase of SL and KL concentrations, respectively for pH 6. At pH 8, the i_{corr} values decreased from 5.81 to 2.47 μA cm^{-2} and 2.6 to 1.93 μA cm^{-2} and the %*IE* increase from 78 to 91% and 82 to 95% with the increase of SL and KL concentrations, respectively. The results indicated that the %*IE* of the SL inhibitor is greater than that of the KL inhibitor. This could be related to the increase of the number of active sites, the electron densities [28], the number of functional groups in the macromolecule of lignin and molecular size [29]. It has been reported that the effectiveness of lignin and its modifications as an inhibitor is due to the increase number of OH and COOH groups in its macromolecule or monomer [30].

Table 3. Polarization parameters of mild steel in 3.5% NaCl without and with various concentrations of SL and KL at pH 6.

	Conc. (ppm)	E_{corr} (mV)	b_a (mV decade^{-1})	b_c (mV decade^{-1})	I_{corr} (μA cm^{-1})	*IE* (%)	θ	v
Blank	-	-676	64.1	1707	28.91	-	-	-
	50	-622	88.2	7842	8.89	79.18	0.791	4.80
	100	-663	82.2	6880	5.78	86.46	0.864	7.39
Soda lignin	200	-674	73.1	1440	4.07	90.47	0.904	10.49
	400	-691	85.6	204	2.67	93.75	0.937	15.99
	800	-718	78.1	173	2.13	95.01	0.950	20.05
	50	-645	10.9	1205	8.15	80.91	0.809	5.24
	100	-657	74.5	1890	5.34	87.49	0.874	8.00
Kraft lignin	200	-661	80.7	6240	4.36	89.79	0.897	9.79
	400	-678	10.7	5460	3.84	91.01	0.910	11.12
	800	-691	95.6	2190	3.16	92.60	0.926	13.51

Table 5 shows the polarization values of the three monomers of lignin on the corrosion of mild steel in 3.5% NaCl. The increasing order of % *IE* is p-cumaric acid and ferulic acid have shown good inhibition due to presence of carboxyl groups in the monomer structure as compared to 4-hydroxybenzaldehyde. It could be assumed, that carboxyl groups had better corrosion protection ability than the hydroxyl groups due to better electron donating ability of carboxyl group to the iron ions.

The effective monomers act as mixed-type inhibitors, indicating that molecules are adsorbed on both sites, but under prominent cathodic oxygen reduction. The corrosion efficiencies of CA and FA were remarkably increased by increasing the monomer concentration unlike HB. The polarity of monomers is related to type and electron donating of functional groups which are attached. Generally, the higher polarity follows a lower Tafel's slopes at polarization curves.

Table 4. Polarization parameters of mild steel in 3.5% NaCl without and with various concentrations of SL and KL at pH 8.

	Conc. (ppm)	E_{corr} (mV)	b_a (mV decade^{-1})	b_c (mV decade^{-1})	I_{corr} (μA cm^{-1})	*IE* (%)	*θ*	*v*
Blank	-	-689	72.2	1910	17.75	-	-	-
	50	-744	64.8	5855	5.81	78.87	0.788	7.68
	100	-728	63.0	4990	4.11	81.88	0.818	8.50
Soda lignin	200	-717	65.0	4172	3.24	85.03	0.850	8.77
	400	-703	46.9	2838	2.81	90.00	0.900	12.80
	800	-707	64.2	2378	2.47	91.55	0.915	34.85
	50	-695	88.4	878	6.90	82.03	0.820	5.57
	100	-702	54.0	340	5.35	86.07	0.860	7.18
Kraft lignin	200	-661	99.7	6780	5.51	85.65	0.856	6.97
	400	-737	14.4	1440	2.44	93.65	0.936	15.74
	800	-820	78.3	1920	1.93	94.97	0.949	19.90

On the other hand, less corrosive rate occurred at higher pH levels but there were no significant differences. The inhibition coefficient (*v*) increased when the concentration of inhibitor increased in the corrosive media. It has been reported [31], if the displacement in E_{corr} is over than 85 mV the inhibitor can be seen as a cathodic or anodic type inhibitor and if the displacement of E_{corr} is lower than 85 mV, the inhibitor can be seen as mixed type.

From the polarization curves at pH 6, it is suggested that the utilized inhibitors act as mixed type inhibitors and predominately as cathodic inhibitors at pH 8. The lower corrosion current densities (i_{corr}) with respect to the blank (inhibitor free corrosive media) were achieved by increasing the concentrations of the tested inhibitors.

Table 5. Polarization parameters of mild steel in 3.5% NaCl without and with various concentrations of p-cumaric acid, ferulic acid and hydroxybenzaldehyde.

	Conc. (ppm)	E_{corr} (mV)	b_a (mV decade^{-1})	b_c (mV decade^{-1})	I_{corr} (µA cm^{-2})	*IE* (%)	θ
Blank	-	-692	34.6	408.2	47.7	-	-
	100	-781	88.2	193.5	8.78	81.59	8.16
p-Cumaric acid	200	-743	73.5	146.2	7.62	84.03	8.40
	400	-740	83.5	178.4	5.48	88.51	8.85
	800	-691	88.3	213.5	4.67	90.21	9.02
	100	-742	84.6	151.5	6.59	86.18	8.62
Ferulic acid	200	-734	58.2	183.4	7.78	83.69	8.37
	400	-721	53.6	196.1	5.95	87.53	8.75
	800	-714	60.7	234.5	4.85	89.83	8.98
	100	-761	58.9	177.2	26.16	45.16	4.52
Hydroxybenzaldehyde	200	-754	67.3	363.9	25.73	46.06	4.61
	400	-746	80.9	489.3	24.8	48.01	4.80
	800	-721	73.8	571.5	41.03	13.98	1.40

This behavior confirms an increase in the energy barrier or activation energy of carbon steel dissolution process in corrosive media. The polarization curves show that oxygen is the cathodic reactant in this near neutral solutions. Hydroxide ions which are produced as result of cathodic reaction

$$2H_2O + O_2 + 4e^- \rightarrow 4OH^-$$

And it may attack the steel surface.

3.3 Electrochemical impedance measurements

The impedance behavior of mild steel in 3.5% NaCl without and with various concentrations of SL and KL at pH 6 and 8 are shown in Fig. 4. The impedance parameters such as the charge solution resistance (R_u), transfer resistance (R_{ct}) and double layer capacitance (C_{dl}) are obtained by modeling the equivalent circuit of the electrochemical cell. The impedance at high frequency is related to the ohmic resistances of the corrosion product films and the solution enclosed between the working electrode and the reference electrode (SCE). Polarization resistance (R_p) may include the different types of resistances such as R_{ct}, charge transfer resistance; R_d, diffuse layer resistance; R_a, resistance of accumulated species (corrosion products or any existing molecules or ions); R_f , resistance of film (R_p

$= R_{ct} + R_a + R_d + R_f$*).* But to simplify the calculation they are measured as R_p. This ohmic resistive behavior is valued by a zero degree phase angle between current and potential at high frequency like the constant current (*Z=R=V/I*).

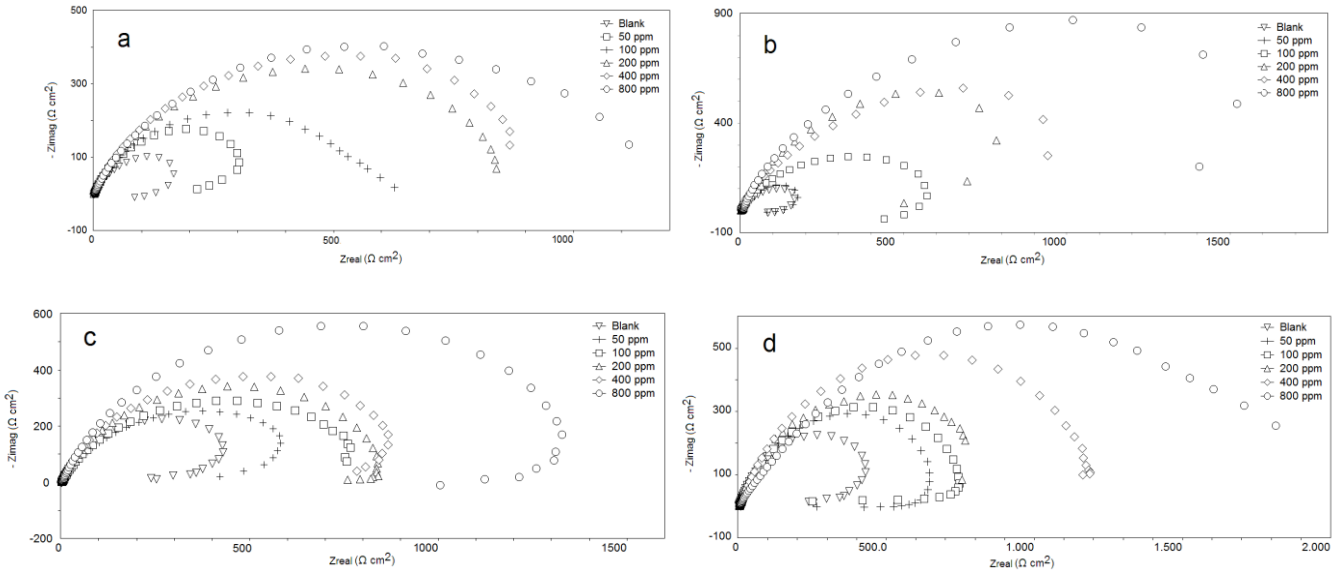

Figure 4. EIS curves of mild steel in 3.5% NaCl with (a) SL, pH 6 (b) KL, pH 6 (c) SL, pH 8 (d) KL, pH 8.

The capacitance value (in electrochemical cells, the Helmholtz Double Layer act as capacitance) can be used for the evaluation of the inhibitor that is adsorbed on the metal base that is affected by either dielectric constant of adsorbed layer or the thickness of the film calculated from Equation (7):

$$C = r\varepsilon_0 \varepsilon \frac{A}{d} \tag{7}$$

where r is the roughness factor of surface, ε_0 is the permittivity of free space that equals to 8.85×10^{-12} F m^{-1}, ε the dielectric constant of the surface film, A the exposed area of the working electrode and d is the average thickness of adsorbed layer, containing the corrosion products and inhibitor protective film.

The constant phase element (CPE) could be modeled as a parallel combination of a pure capacitor and a resistor set in reverse of the angular frequency. The impedance of the CPE is shown as [32]:

$$Z_{CPE} = \frac{1}{Y_0(j\omega)^n} \tag{8}$$

where Y_0 is the admittance or magnitude of the CPE, j is a complex number equal $\sqrt{-1}$, ω is $2\pi f$ (f is frequency) , n is the phase shift value = $\alpha/(\pi/2)$; α is the phase angle ($-1 \leq n \leq 1$). Z_{CPE} represents different functions in a circuit, for $n = 0$ it can be modeled as a resistance with $R = Y^{-1}$, for $n = 1$ a capacitance with $C = Y$, for $n = 0.5$ a Warburg element and for $n = -1$ is an inductive with $L = Y^{-1}$ (L is inductive capacity).

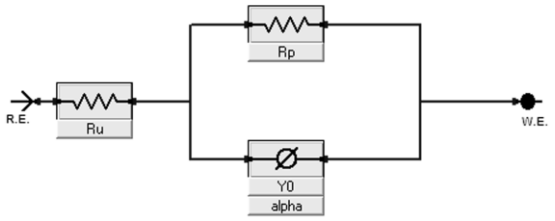

Figure 5. Equivalent circuit used to fit the impedance measurements (solution resistance (R_u), a constant phase element (φ) and a charge transfer or polarization resistance (R_p)) via Echem Analyst software.

The high frequency (HF) loops have depressed semicircular appearance, $0.5 \leq n \leq 1$, which is usually referred to as frequency dispersion and attributed non-homogeneity or the roughness of the solid metal surface [33]. Consequently, the equivalent circuit described in Fig. 5 with a constant phase element, CPE, is used to fit our experimental results. In this case, the phase shift (n) was close to 1 so it can be substituted for the capacitance instead of the CPE; therefore, the C_{dl} can be calculated instead of Y in the equivalent circuit. The C_{dl}, for a circuit including a CPE can be calculated from Eqs. (9 or 10) [34]:

$$C_{dl} = Y_0(\omega_{max})^{n-1} \quad (9)$$

or

$$C_{dl} = \frac{1}{2\pi f_{max} R_{ct}} \quad (10)$$

where $\omega_{max} = 2\pi f_{max}$; f_{max} is the frequency of a point in the Nyquist plot which has the maximum imaginary part of the impedance.

From the values of R_{ct} or polarization resistance (R_p), the inhibition efficiencies are calculated by Equation (11) and tabulated in Table 6 and 7 [9]:

$$\%IE = \frac{R_p - R_p^0}{R_p} \times 100 \quad (11)$$

where R_p^0 and R_p are the polarization resistances for uninhibited and inhibited solutions, respectively.

Table 6. EIS parameters of mild steel in 3.5% NaCl with and without various concentrations of SL and KL at pH 6.

	Conc. (ppm)	R_u (Ω cm^2)	R_p (Ω cm^2)	*n*	C_{dl} (F cm^{-2})	*IE* (%)	*θ*
Blank	-	1.83	234	0.895	2.47E-02	-	-
	50	1.12	323	0.911	5.95E-03	27.61	0.276
	100	1.81	601	0.874	2.11E-03	61.09	0.610
Soda lignin	200	1.08	868	0.868	2.79E-03	73.04	0.730
	400	0.83	1083	0.925	5.53E-03	78.39	0.783
	800	1.01	1234	0.885	7.57E-03	81.03	0.810
	50	1.28	403	0.905	7.69E-03	41.9	0.419
	100	2.38	645	0.845	3.11E-03	63.7	0.637
Kraft lignin	200	1.92	1347	0.872	1.49E-03	82.6	0.826
	400	2.51	1356	0.875	4.67E-03	82.7	0.827
	800	3.70	2123	0.866	2.98E-03	89.0	0.890

The Nyquist plots in Fig. 4 indicated capacitive loops at high frequencies in the absence and presence of lignin, signifying that the corrosion process is mainly controlled by a charge transfer process. Inductive loops can be observed at low frequencies in the absence and at certain concentrations of lignin. In this case, the corroding process could occur in two steps, first oxidation of metal or anodic dissolution under charge transfer process and continued by the relaxation process which can be achieved by the adsorption of H^+_{ads} or corrosion products or molecule of inhibitors or re-dissolution of protective film at low frequencies onto the metal surface [35]. Table 6 shows that the R_{ct} values increased from 243 Ω cm^2 for blank sample at pH 6 to the maximum values of 1234 and 2123 Ω cm^2, respectively, and C_{dl} values decreased from 2.47×10^{-2} F cm^{-2} to 7.57×10^{-3} and 2.98×10^{-3} F cm^{-2} with the increase of the SL and KL inhibitor concentrations, respectively. The diameters of the capacitive loop increased with increasing of SL or KL concentrations in media, which can be attributed to increasing coverage of electrode surface by inhibitor. In addition, the adsorption of inhibitor to forming the protective film increased the electrical resistance between metal and corrosive media.

The decrease in C_{dl} values indicates that the adsorption of SL and KL molecules on the mild steel surface and the corrosion process involved is an activation controlled reaction. Decrease in the C_{dl} values with increase of the inhibitor concentrations could be related to the decrease in the local dielectric constant and/or an increase in the thickness of the electrical double layer that is attributed to the slightly permeable water molecules via the organic molecules onto the metal surface.

Table 7. EIS parameters of mild steel in 3.5% NaCl with and without various concentrations of SL and KL at pH 8.

	Conc. (ppm)	R_u (Ω cm^2)	R_p (Ω cm^2)	*n*	C_{dl} (F cm^{-2})	*IE* (%)	*θ*
Blank	-	2.01	517	0.865	2.44E-03	-	-
	50	1.16	743	0.732	2.70E-03	30.4	0.304
	100	2.88	833	0.766	3.02E-03	38.0	0.380
Soda lignin	200	1.07	922	0.802	8.61E-03	44.0	0.440
	400	0.74	1045	0.815	1.92E-03	50.5	0.505
	800	0.52	1432	0.729	1.11E-03	63.9	0.639
	50	10.15	720	0.857	8.77E-03	28.2	0.282
	100	5.79	816	0.785	1.95E-03	36.6	0.366
Kraft lignin	200	2.87	988	0.761	3.21E-03	47.7	0.477
	400	9.07	1258	0.808	1.00E-03	58.9	0.589
	800	4.21	1996	0.859	2.52E-03	74.1	0.741

3.4 Adsorption isotherm

Inhibition effects are based on the adsorption of molecules onto the metal surface to form an impermeable protective film and shielding it from the corrosive media. On the other hand, the adsorbed molecules can combine with the oxide layer on the metal (rust deposited) and react chemically to produce a more protective surface network and change the structure. The adsorption mechanism of organic compounds performs either directly, on the basis of donor-acceptor interactions between relatively loosely bound electrons such as in anions and organic molecules and/or the heterocyclic compound which has lone pair electrons or the π-electrons with the vacant d-orbitals of iron atoms of metal [36]. Some parameters of organic molecules such as molecule size, number of functional groups, polarity that contributed to the formation of the strongest bonding or rate of adsorptions of inhibitor compounds onto the surface could affect the adsorption mechanism or inhibition action.

In order to consider the adsorption process of inhibitor compounds on the metal surface, Langmuir, Temkin and Frumkin adsorption isotherms were tested according to the following equations [37, 38]:

$$\text{Langmuir: } \frac{C_{inh}}{\theta} = \frac{1}{K_{ads}} + C_{inh} \quad \text{or} \quad \frac{\theta}{1-\theta} = KC_{inh} \tag{12}$$

Where θ is the surface coverage coefficient, K_{ads} is the equilibrium constant of the adsorption, C_{inh} is the inhibitor concentration and g is the adsorbate interaction parameter.

Assuming that the corrosion inhibition is due to the adsorption of lignins, the degree of surface coverage (θ) for different concentrations of SL and KL lignin in 3.5% NaCl was measured from weight loss measurements. To determine which adsorption isotherm has the best fitting of the surface coverage and to calculate the free-energy of adsorption, different isotherms were tested. The well fitted data with the highest regression coefficient close to 1 was obtained via Langmuir's isotherm as can be seen in Fig. 6.

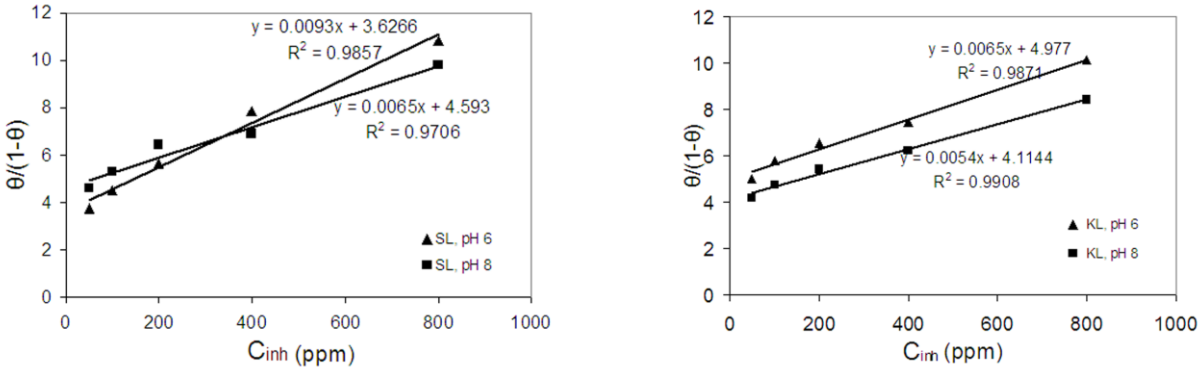

Figure 6. Langmuir adsorption plot for on Mild steel at 3.5% NaCl and pH 6 and 8 obtained in the 25 °C temperature for 240 hours (a) soda lignin and (b) Kraft lignin.

It shows the linear curves when $\theta/(1-\theta)$ versus C_{inh} were plotted at two levels of pH and the linear equation and regression distribution. This linear trend confirms that SL and KL inhibitors obey Langmuir's adsorption isotherm at both pH levels at 25 °C. The value of the adsorption–desorption equilibrium constant, K_{ads}, was determined from the slope of the isotherm line (L mg^{-1}). It can be seen from Fig. 6 that SL (especially at low pH) has the higher adsorption ability compared to KL due to the higher adsorption equilibrium constant which reflects the high adsorption on the metal surface. The free energy of adsorption, ΔG_{ads} of inhibitors on a mild steel surface can be measured with the following equation [10]:

$$\Delta G_{ads} = -RT \ln(C_{water}.K_{ads}) \tag{13}$$

where C_{water} is the water concentration (10^6 mg L^{-1}), R is the universal gas constant and T is the absolute temperature. The adsorption parameter values from this isotherm are tabulated in Table 8. It is seen from the table that the results were plotted linearly with very good correlation coefficients and K_{ads} values decreases with increasing pH and SL has better adsorption than KL. Physisorption are

electrostatic interactions between organic adsorbed compounds and the charged metal, which has ΔG_{ads} values around and/or lower than −20 kJ mol^{-1}.

Table 8. Data from Langmuir's isotherm for SL and KL on Mild steel at 3.5% NaCl and pH 6 and 8 obtained at the room temperature for 240 hours.

Inhibitor	K_{ads}(L mg^{-1})	ΔG_{ads} (kJ mol^{-1})	R^2
Soda, pH6	0.0093	-23.4005	0.9857
Soda, pH8	0.0065	-22.4832	0.9706
Kraft, pH6	0.0065	-22.4832	0.9871
Kraft, pH8	0.0054	-22.0084	0.9908

Those having ΔG_{ads} values around −40 kJ mol^{-1} or higher are chemisorbed via electron transfer to form the co-ordinate bonds from the organic molecules to the metal surface [39]. It has been revealed that the adsorption of the inhibitors on anodic sites follow the chemical adsorption and adsorption on cathodic sites due to the electrostatic attraction [40].

The values of ΔG_{ads} show that the molecules of lignin (SL and KL) were adsorbed first physically and continued with chemical adsorption on the mild steel surface. It has been assumed in the Langmuir's isotherm that adsorbed molecules do not interact with each other, but this is not real in large organic molecules (such as lignin) having polar atoms or aromatic groups. Increase the number of electron donator functional groups promote adsorption and corrosion inhibition. The most probable and dominant adsorption sites were found in the vicinity of the phenolic groups. Such molecules are adsorbed by mutual repulsion or attraction on the cathodic and anodic sites of the metal surface. Similar observation has been reported by former studies [41].

3.5 FT-IR studies

The FT-IR spectra of mild steel exposed in solutions containing 3.5% NaCl with and without high concentrations of KL at pH 6 and 8 are shown in Fig. 7. The principal FTIR peaks of the various iron oxides and oxyhydroxides [MO_xOH_y] such as lepidocrocite (γ-FeOOH) are around 1150, 1022, 750 and 474 cm^{-1} [42], goethite (α-FeOOH) at 900 cm^{-1} and the shoulder at 800 cm^{-1} [43] and magnetite (Fe_3O_4) 571 at 566 cm^{-1} [44]. Fig. 7(a) shows the peaks at 1022 and 474 cm^{-1} designating the presence of lepidocrocite and 566 and 571 cm^{-1} belonging to magnetite in blank samples at pH 6 and 8. Upon treatment of steel samples with lignin, ferric-lignin peaks at 1117, 1217, 1462, 1512 and 1614 cm^{-1} were evident and the lepidocrocite peak at 1022 cm^{-1} reduced.

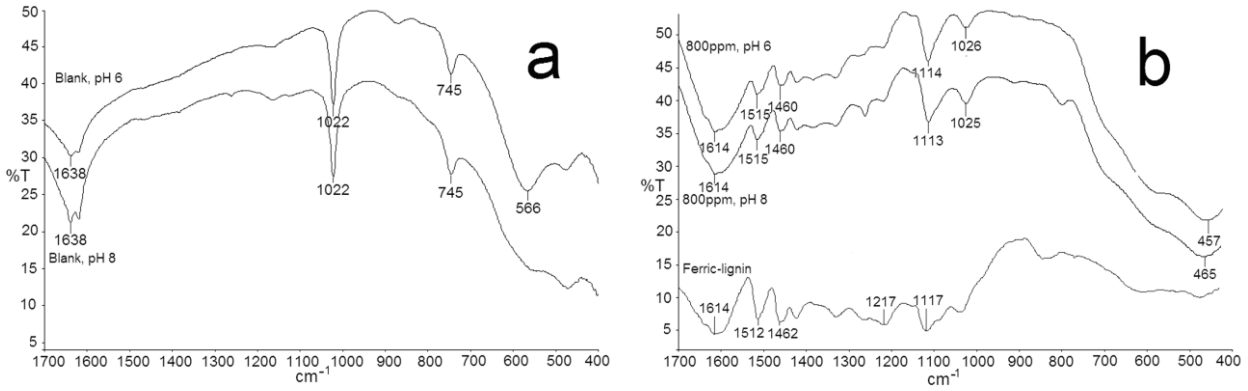

Figure 7. FT-IR spectra of mild steel samples immersed in 3.5% NaCl (a) Blank (b) 800ppm of Kraft lignin at pH 6 and 8 at 20 °C for 240 hours.

3.6 Surface morphology analysis

Fig. 8 shows the surface morphology of corroded samples in 3.5% NaCl solution without inhibitors at pH 6 and 8 at low (1000x) and high magnifications (6000x).

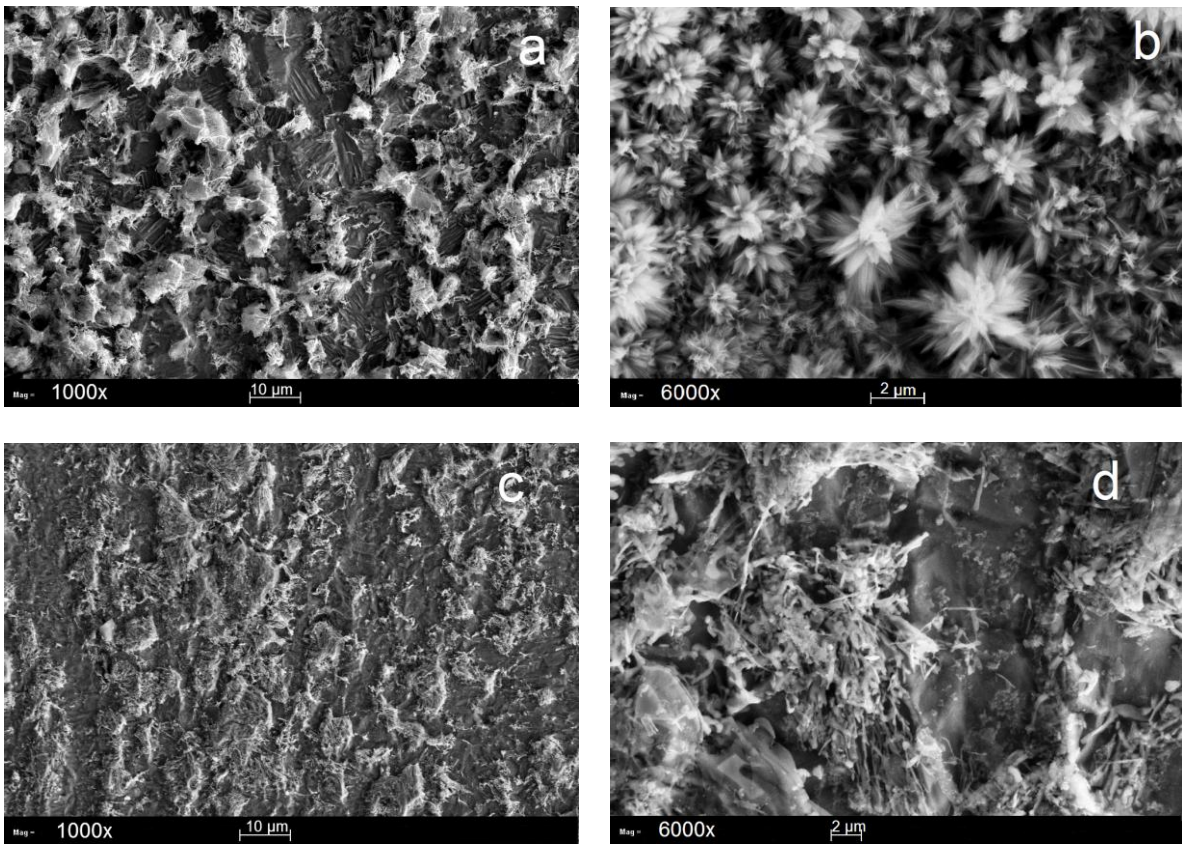

Figure 8. SEM micrographs of mild steel corroded surface immersed in 3.5% NaCl without inhibitor for 240 h, (a) 1000x, at pH 6 (b) 6000x, pH 6, (c) 1000x, pH 8 (d) 6000x, pH 8.

At low resolution, the homogeneous attack and corrosion products throughout the surface of tested specimens at both pH levels can be observed. At higher magnification (Fig. 8b), flower-like structures, typical of rust components could be observed. Generally, the ferrite-pearlite structures are

found in low carbon steels. The ferrite can be corroded preferentially, so the corrosion products are deposited on top of the pearlite. Smaller pits and morphology of formed rust on the surface of corroded samples in pH 8 validate the lower corroding action compared to pH 6. The presence of carbides (shown as black area in Fig. 8a) were detected in the corrosion products as residual matter from the corrosion reaction [45]. It has been reported that cementite is the preferable site for a cathodic reaction and ferrite (α-iron) as an anodic reaction [46].

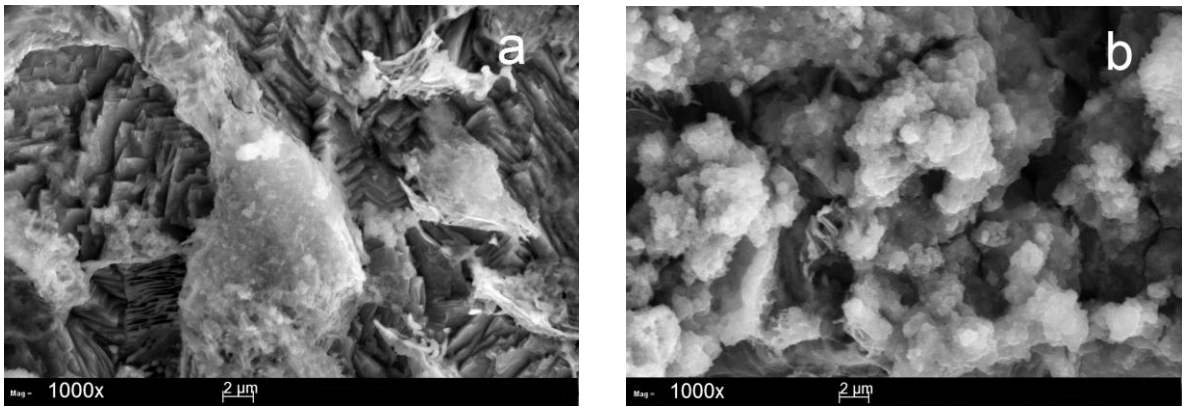

Figure 9. SEM micrographs of mild steel corroded surface immersed in 3.5% NaCl with inhibitor for 240 h, (a) brushed surface at pH 6 and (b) brushed surface at pH 8.

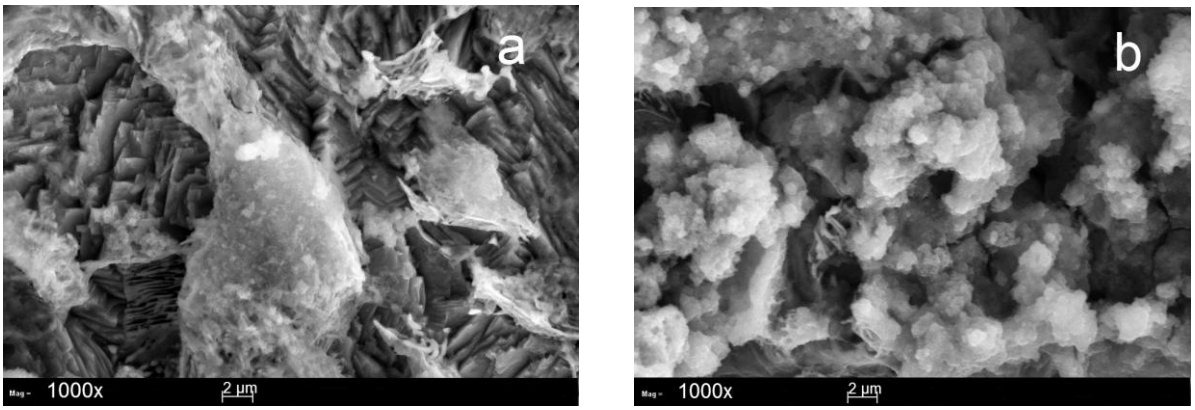

Figure 10. SEM micrographs of mild steel corroded surface immersed in 3.5% NaCl with inhibitor for 240 h at pH 6, (a) un-brushed surface at pH 6 and (b) un-brushed surface at pH 8.

Fig. 9 shows the morphology of surfaces that were brushed slightly (to study the morphology of formed rust) and Fig. 10 shows un-brushed (to study the formation of new compounds on the surfaces), respectively. They are corresponding to samples kept in contact with the inhibited solution of 3.5% NaCl solution containing 800 ppm of Kraft lignin as a corrosion inhibitor for 240 hours at pH 6 and 8 in an aerated situation at 25 °C. These specimens show the formation of an adsorbed protective film or formation of ferric-lignin as a barrier shield onto the exposed area. Fig. 9b shows the surface treated with an inhibitor at pH 8 that shows no new phase such as ferric-lignin or may be other

complexes formed which may be due to the solubility tendency of lignin at high pH. But, in Fig. 9a some residual of deposited ferric-lignin can be seen. On closer observation, lepidocrocite reduction occurred in the cementite background.

The ferric-lignin, as new formed compound is strongly exhibited in Fig. 10 at both pH levels due to the un-brushed immersed samples after treatment. Adsorption is the initial mechanism of the inhibiting process and the new compound covering the corroded steel surface with the initial oxides acting as a protective barrier to prevent further penetration of Cl^- into the corrosive substrates. The covered oxide layers with the ferric-lignin compound were clearly shown in Fig. 10a. These results can support the electrochemical measurements achieved during the corrosion tests. Corrosion products strictly depend on the steel microstructure and the molecular structure and bonding of the employed inhibitor. The SL exhibited similar morphology to that of KL.

These observations are supported by the EDX results that show the reduced content of oxygen for samples that were immersed in SL or KL compared to the blank solution of 3.5% of NaCl. This can be attributed to the protected film of adsorbed lignin onto the metal surface that inhibits the oxidation and corrosion.

4. CONCLUSION

- Soda and Kraft lignin are good inhibitors for mild steel corrosion in 3.5% NaCl at both pH 6 and 8 at 25 °C. SL and KL gave a maximum efficiency of 89 and 87% at pH 6 and 92 and 90% at pH 8, respectively. The SL exhibited better inhibition compared to KL at both pH levels and lower efficiency at a higher pH.
- It is confirmed that SL and KL are mixed type inhibitors from the polarization study and they obey Langmuir's adsorption isotherm at both pH levels and at 25 °C.
- The p-cumaric acid, ferulic acid and 4-hydroxybenzaldehyde as selected monomers of lignin have shown inhibitory action with different levels of protection depending on the type and number of functional groups present in the molecule.
- Scanning Electron Microscopy also confirms that the morphology structure of mild steel is less corroded in a solution containing SL compared to the solution containing KL at both pH levels. The new compound presumably ferric-lignin was formed on the surface of mild steel and prohibited further corroding processes. The EDX results showed that the oxygen content has been reduced with the increase of lignins concentrations.
- FTIR study confirms the reduction of rust particularly, lepidocrocite on a surface of mild steel as well as the formation of the ferric-lignin.

ACKNOWLEDGMENT

The authors are indebted to Universiti Sains Malaysia for financial support of this project through Research University Grant scheme (1001/PKIMIA/854002).

References

1. A.A. Rahim, E. Rocca, J. Steinmetz, M.J. Kassim, R. Adnan and M. Sani Ibrahim, *Corros. Sci.*, 49 (2007) 402.
2. A.Y. El-Etre, *Corros. Sci.*, 43 (2001) 1031.
3. A.Y. El-Etre, *Corros. Sci.*, 45 (2003) 2485.
4. A.Y. El-Etre and M. Abdallah, *Corros. Sci.*, 42 (2000) 731.
5. A.M. Abdel-Gaber, B.A. Abd-El-Nabey and M. Saadawy, *Corros. Sci.*, 51 (2009) 1038.
6. A.M. Abdel-Gaber, B.A. Abd-El-Nabey, I.M. Sidahmed, A.M. El-Zayady and M. Saadawy, *Corros. Sci.*, 48 (2006) 2765.
7. J.R. Davis, *Corrosion: Understanding the basic*, ASM International, USA (2000).
8. M. Behpour, S.M. Ghoreishi, N. Soltani, M. Salavati-Niasari, M. Hamadanian and A. Gandomi, *Corros. Sci.*, 50 (2008) 2172.
9. N. Soltani, M. Behpour, S.M. Ghoreishi and H. Naeimi, *Corros. Sci.*, 52 (2010) 1351.
10. R. Solmaz, G. Kardas, B. YazIcI and M. Erbil, *Colloids Surf. A: Physicochemical and Engineering Aspects*, 312 (2008) 7.
11. A.L. Korich, K.M. Clarke, D. Wallace and P.M. Iovine, *Macromolecules*, 42 (2009) 5906.
12. E.L.J. Stuart, D.G. Jerry and J.M. Timothy, *Kirk-Othmer Encyclopedia of Chemical Technology*, (2001).
13. M.N. Mohamad Ibrahim, M.Y.N. Nadiah and H. Azian, *J. Appl. Sci.*, 6 (2006) 292.
14. Y.L. Zhu, X.P. Guo and Y.B. Qiu, *Corros. Eng., Sci. Technol.*, 45 (2010) 442.
15. N. Andreeva, L. Kazanskii, I. Selyaninov, Y. Kuznetsov and V. Ostrovskii, *Prot. Met. Phys. Chem. Surf.*, 45 (2009) 806.
16. M.N. Mohamad Ibrahim, M.R. Ahmed-Haras, C.S. Sipaut, H.Y. Aboul-Enein and A.A. Mohamed, *Carbohydr. Polym.*, 80 (2010) 1102.
17. M. Mahdavian and S. Ashhari, *Electrochim. Acta*, 55 (2010) 1720.
18. A.Y. Musa, A.A.H. Kadhum, M.S. Takriff, A.R. Daud, S.K. Kamarudin and N. Muhamad, *Corros. Eng., Sci. Technol.*, 45 (2010) 163.
19. P.C. Okafor, E.E. Ebenso and U.J. Ekpe, *Int. J. Electrochem. Sci.*, 5 (2010) 978.
20. S.A. Lajevardi, L. Mosalaeepour and T. Shahrabi, *Corros. Eng., Sci. Technol.*, 45 (2010) 295.
21. A.Musa, A. Mohamad, A. Kadhum and Y. Tabal, *J. Mater. Eng. Perform.*, 20 (2011) 394.
22. P.K. Gogoi and B. Barhai, *Int. J. Electrochem. Sci.*, 6 (2011) 136.
23. F. Mansfeld, *Corrosion Mechanisms*, Marcel Dekker, New York (1987).
24. M. Elayyachy, M. Elkodadi, A. Aouniti, A. Ramdani, B. Hammouti, F. Malek and A. Elidrissi, *Mater. Chem. Phys.*, 93 (2005) 281.
25. M.G. Hosseini and M.R. Arshadi, *Int. J. Electrochem. Sci.*, 4 (2009) 1339.
26. S.P. Arredondo-Rea, R. Corral-Higuera, M.A. Neri-Flores, J.M. Gómez-Soberón, F. Almeraya-Calderón, J.H. Castorena-González and J.L. Almaral-Sánchez, *Int. J. Electrochem. Sci.*, 6 (2011) 475.
27. N.O. Obi-Egbedi, K.E. Essien, I.B. Obot and E.E. Ebenso, *Int. J. Electrochem. Sci.*, 6 (2011) 913.
28. B.M. Praveen and T.V. Venkatesha, *Int. J. Electrochem. Sci.*, 4 (2009) 267.
29. A.A. El-Shafei, S.A. Abd El-Maksoud and A.S. Fouda, *Corros. Sci.*, 46 (2004) 579.
30. Y.N. Forostyan and M. Prosper, *Chem. Nat. Compd.*, 19 (1983) 358.
31. A.K. Satapathy, G. Gunasekaran, S.C. Sahoo, K. Amit and P.V. Rodrigues, *Corros. Sci.*, 51 (2009) 2848.
32. I.B. Obot, N.O. Obi-Egbedi, S.A. Umoren and E.E. Ebenso, *Int. J. Electrochem. Sci.*, 5 (2010) 994.
33. A.V. Benedeti, P.T.A. Sumodjo, K. Nobe, P.L. Cabot and W.G. Proud, *Electrochim. Acta*, 40 (1995) 2657.
34. C.H. Hsu and F. Mansfeld, *CORROSION*, 57 (2001) 747.
35. Y. Zuo, R. Pang, W. Li, J.P. Xiong and Y.M. Tang, *Corros. Sci.*, 50 (2008) 3322.

36. M. Ehteshamzadeh, A.H. Jafari, E. Naderi and M.G. Hosseini, *Mater. Chem. Phys.*, 113 (2009) 986.
37. I.Langmuir, *J. Amer. Chem. Soci.*, 38 (1916) 2221.
38. L. Tang, X. Li, L. Li, G. Mu and G. Liu, *Mater. Chem. Phys.*, 97 (2006) 301.
39. G. Moretti, F. Guidi and G. Grion, *Corros. Sci.*, 46 (2004) 387.
40. S. Sathiyanarayanan, C. Marikkannu and N. Palaniswamy, *Appl. Surf. Sci.*, 241 (2005) 477.
41. M.M. Solomon, S.A. Umoren, I.I. Udosoro and A.P. Udoh, *Corros. Sci.*, 52 (2010) 1317.
42. H. Antony, L. Legrand, L. Maréchal, S. Perrin, P. Dillmann and A. Chaussé, *Electrochim. Acta*, 51 (2005) 745.
43. H. Antony, S. Peulon, L. Legrand and A. Chaussé, *Electrochim. Acta*, 50 (2004) 1015.
44. M. Gotic and S. Music, *J. Mol. Struct.*, 834-836 (2007) 445.
45. L.D. Paolinelli, T. Pérez and S.N. Simison, *Corros. Sci.*, 50 (2008) 2456.
46. E. Naderi, M. Ehteshamzadeh, A.H. Jafari and M.G. Hosseini, *Mater. Chem. Phys.*, 120 (2010) 134